Location of a Cation-Binding Site in the Loop between Helices F and G of Bacteriorhodopsin as Studied by ^{13}C NMR

Satoru Tuzi,* Satoru Yamaguchi,* Michikazu Tanio,* Hidemasa Konishi,* Sayuri Inoue,* Akira Naito,* Richard Needleman,# Janos K. Lanyi,§ and Hazime Saitô*

*Department of Life Science, Himeji Institute of Technology, Harima Science Garden City, Kamigori, Hyogo, Japan 678-1297; #Department of Biochemistry, Wayne State University, Detroit, Michigan 48201 USA; and §Department of Physiology and Biophysics, University of California, Irvine, California 92697-4560 USA

ABSTRACT The high-affinity cation-binding sites of bacteriorhodopsin (bR) were examined by solid-state ^{13}C NMR of samples labeled with [3-^{13}C]Ala and [1-^{13}C]Val. We found that the ^{13}C NMR spectra of two kinds of blue membranes, deionized (pH 4) and acid blue at pH 1.2, were very similar and different from that of the native purple membrane. This suggested that when the surface pH is lowered, either by removal of cations or by lowering the bulk pH, substantial change is induced in the secondary structure of the protein. Partial replacement of the bound cations with Na^+, Ca^{2+}, or Mn^{2+} produced additional spectral changes in the ^{13}C NMR spectra. The following conclusions were made. First, there are high-affinity cation-binding sites in both the extracellular and the cytoplasmic regions, presumably near the surface, and one of the preferred cation-binding sites is located at the loop between the helix F and G (F-G loop) near Ala^{196}, consistent with the 3D structure of bR from x-ray diffraction and cryoelectron microscopy. Second, the bound cations undergo rather rapid exchange (with a lifetime shorter than 3 ms) among various types of cation-binding sites. As expected from the location of one of the binding sites, cation binding induced conformational alteration of the F-G interhelical loop.

INTRODUCTION

The retinal chromophore in bacteriorhodopsin (bR), the light-driven proton pump in the purple membrane of *Halobacterium salinarium*, is covalently linked to Lys^{216} through a protonated Schiff base. In the light-adapted unphotolyzed state at neutral pH its absorbance maximum is at 568 nm. Upon excitation with light, bR undergoes a cyclic photoreaction with intermediates J, K, L, M, N, and O, which are sequentially formed before recovery of the initial state (Ovchinnikov, 1982; Stoeckenius and Bogomolni, 1982; Mathies et al., 1991; Lanyi, 1993, 1997). During this photocycle, a proton is released on the extracellular side from the proton release chain (Glu^{204}, Glu^{194}, and a bound water) when the M intermediate is formed (Brown et al., 1995; Dioumaev et al., 1998; Luecke et al., 1998), and subsequently proton uptake occurs on the cytoplasmic surface during the O-to-bR transition. The result of the photoreaction is the transport of a proton from the cytoplasmic to the extracellular side. Lowering the pH of the medium or removal of cations from the purple membrane (which increases the apparent pK of Asp^{85}) shifts the absorbance maximum from 568 nm to 604 nm, and bR forms the blue membrane, hereafter referred to as acid or deionized blue membrane, respectively (Moore et al., 1978; Mowery et al., 1979; Fischer and Oesterhelt, 1979; Kimura et al., 1984). The blue membrane has an altered photocycle and no proton transport activity (Mowery et al., 1979; Chang et al., 1986; Dunach et al., 1987). Removal of a negative charge of Asp^{85} near the Schiff base, by either protonation or site-specific mutagenesis, leads to red shift of the absorption maximum. The removal of the negative charge of Asp^{85} as the Schiff base counterion is directly involved in the red shift of the absorption maximum in the acid and deionized blue membrane (Subramaniam et al., 1990; Zhang et al., 1993).

The presence of specific cation-binding sites was initially proposed in relation to the alterations of the color and function of bR (Chang et al., 1985; Ariki and Lanyi, 1986). Although Szundi and Stoeckenius demonstrated that lowered surface pH, induced by removal of surface-bound cations, can explain the purple-to-blue transition (Szundi and Stoeckenius, 1987, 1989), a variety of experimental evidence suggested more specific cation binding. Potentiometric titration studies of deionized membrane, using a Ca^{2+}-specific electrode, have demonstrated two distinctive categories of cation-binding sites: two high-affinity cation binding sites and four to six low-affinity sites (Zhang et al., 1992, 1993; Zhang and El-Sayed, 1993; Yang and El-Sayed, 1995; Yoo et al., 1995). The binding of cation to the second of the two high-affinity sites had been proposed to correlate with the color change (Ariki and Lanyi, 1986; Zhang et al., 1992), and three to five of the low-affinity sites had been shown to be eliminated upon removal of the C-terminus (Zhang and El-Sayed, 1993). Titration studies using fluorescence measurements (Sweetman and El-Sayed, 1991; Wu and El-Sayed, 1994a, 1994b), radioactive cations (Dunach et al., 1988b), and electron spin resonance (Dunach et al., 1987) have yielded results consistent with titration studies with a Ca^{2+} electrode. In addition, direct observa-

Received for publication 30 June 1998 and in final form 14 November 1998.

Address reprint requests to Dr. Hazime Saitô, Department of Life Sciences, Himeji Institute of Technology, Harima Science Garden City, Kamigori, Hyogo 678-12, Japan. Tel.: 81-7915-8-0181; Fax: 81-7915-8-0182; E-mail: saito@sci.himeji-tech.ac.jp.

0006-3495/99/03/1523/09 $2.00

tion of bound cations by electron diffraction using Pb^{2+}-regenerated purple membrane (Mitra and Stroud, 1990) and an emission decay measurement of bound Eu^{3+} (Corcoran et al., 1987) have shown, respectively, six cation-binding sites partially occupied by two Pb^{2+} ions per bR and three different kinds of binding sites whose binding constants are comparable. Nevertheless, the location of the cation-binding sites and the associated conformational change due to cation binding are as yet unclear.

We have demonstrated earlier that the conformational features of bR can be suitably analyzed by means of conformation-dependent ^{13}C chemical shifts of [3-^{13}C]alanine residues as intrinsic probes (Tuzi et al., 1993, 1994, 1996a,b; Yamaguchi et al., 1998; Tanio et al., 1998). In particular, the C_β ^{13}C chemical shift of Ala residues turned out to be determined only by the torsion angles ϕ and φ and can be utilized to investigate the local conformation of the protein backbone (Saitô, 1986; Saitô and Ando, 1989). We also utilized here [1-^{13}C]Val signals as probes to observe local conformations. In this study, we report on how the conformation of bR is changed between the blue and purple membranes and how the bound cations interact with the protein, by means of solid-state ^{13}C NMR spectroscopy. We found that the purple-to-blue transition induces a drastic conformational change, and it is caused mainly by the lowered surface pH of the blue membrane. Using Na^+-regenerated purple membrane at neutral pH prepared from the deionized blue membrane, we examined effects of the replacements of bound cations with Na^+, Ca^{2+}, and Mn^{2+} on the ^{13}C NMR spectra, and found high-affinity cation-binding sites on both the cytoplasmic and extracellular sides of bR. Rapid exchange among the cation-binding sites was observed for bound Mn^{2+}. This suggests that the binding sites are located near the surface of the protein, where the bound cations have easy access to the medium. Finally, we identified one of the cation-binding sites located on the extracellular surface at the F-G interhelical loop from the spectral changes at Ala^{126} and Ala^{196} as a result of replacement of Ca^{2+} with Mn^{2+} in the purple membrane.

MATERIALS AND METHODS

Sample preparation

[3-^{13}C]-L-alanine ([3-^{13}C]Ala) and [1-^{13}C]-L-valine ([1-^{13}C]Val) were purchased from CIL (Andover, MA) and used without further purification. *Halobacterium salinarium* strain S9 was grown in the TS medium of Onishi et al. (1965), in which unlabeled L-alanine or L-valine was replaced with [3-^{13}C]Ala or [1-^{13}C]Val, respectively. In a similar manner, we labeled the mutant strains A126G (Ala^{126} replaced with Gly), A196G (Ala^{196} replaced with Gly), and E194Q (Glu^{194} replaced with Gln) with [3-^{13}C]Ala or [1-^{13}C]Val. Purple membranes containing bR were isolated by the method of Oesterhelt and Stoeckenius (1974). The samples were finally resuspended in 5 mM HEPES buffer (pH 7.0) containing 10 mM NaCl and 0.025% NaN_3. To prepare acid blue membrane, the purple membrane was resuspended in distilled water, and the pH of the suspension was adjusted to 1.2 with HCl. To prepare deionized blue membrane, purple membrane resuspended in distilled water was treated with cation exchange resin Dowex 50W-X8 until the absorption maximum of the chromophore shifted from 568 nm to 603 nm. The deionized membrane was washed twice with high-purity water (resistivity 18 MΩ·cm) and then resuspended in the same. The pH of the deionized membrane suspension was 4. Adjustment of the bulk pH of the deionized membrane suspension to 7.0 was carried out by titration with 0.01 N NaOH. The final concentration of Na^+ was 400-1400 μM. To prepare Ca^{2+}- or Mn^{2+}-treated membranes, $CaCl_2$ or $MnCl_2$ was added to the deionized membrane suspension, respectively, immediately after the pH was adjusted to 7.0, and the pH was then readjusted to 7.0. The final concentration of Ca^{2+} was 5 μM, and those of Mn^{2+} were 5 and 30 μM. Mole ratios of these cations to bR in the suspensions containing 5 μM and 30 μM cations were ~1/10 and ~1/2, respectively. The membranes thus prepared were concentrated by centrifugation and placed in a 5 mm o.d. zirconia pencil-type rotor for magic angle spinning.

Measurements of ^{13}C NMR spectra

High-resolution solid-state ^{13}C NMR spectra were recorded in the dark on a Chemagnetics CMX-400 NMR spectrometer, by cross-polarization–magic angle spinning (CP-MAS) and single pulse excitation dipolar decoupled magic angle spinning (DD-MAS) methods. The spectral width, acquisition time, and repetition time for CP-MAS and DD-MAS experiments were 40 kHz, 50 ms, and 4 s, respectively. The contact time for the CP-MAS experiment was 1 ms. Free induction decays were acquired with 2 K data points and Fourier-transformed as 16 K data points after 14 K data points were zero-filled. The $\pi/2$ pulses for carbon and protons were 5.0 μs, and the spinning rates were 2.6–4 kHz. A resolution enhancement was performed by the method of Gaussian multiplication. Transients were accumulated 7,000–12,000 times until a reasonable signal-to-noise ratio was achieved. The ^{13}C chemical shifts were referred to the carboxyl signal of glycine (176.03 ppm from tetramethylsilane (TMS)) and then expressed as relative shifts from the value of TMS.

RESULTS

Assignments of [3-^{13}C]Ala-bR signals

Fig. 1 compares the ^{13}C NMR spectra of [3-^{13}C]Ala-bR at neutral pH by DD-MAS and CP-MAS. The spectra contain, respectively, 10 and 12 resolved peaks under improved

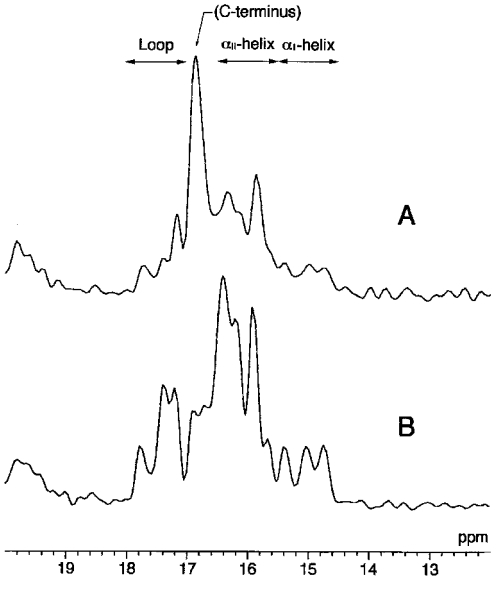

FIGURE 1 Comparison of DD-MAS (*A*) and CP-MAS (*B*) ^{13}C NMR spectra of [3-^{13}C]Ala-bR (pH 7.0) under improved spectral resolution.

spectral resolution, in contrast to earlier spectral resolutions that yielded up to seven peaks only (Tuzi et al., 1996a,b; Yamaguchi et al., 1998). The peak positions in this case are consistent with those in the previous studies, but those at 17.3, 16.4, and 14.8 ppm split into doublets. The "regio-specific assignment" of peaks for the α_I- and α_{II}-helices and loops was made with reference to the previous data (Tuzi et al., 1994, 1996a; Yamaguchi et al., 1998), as indicated above the peaks in Fig. 1. It is noteworthy that two peaks (16.90 and 16.70 ppm) are buried beneath the intense signal at 16.87 ppm from the C-terminus domain taking random coil conformation in the DD-MAS spectrum, whereas their presence is more evident in the CP-MAS measurement, where they are free from the intense peak due to rapid conformational fluctuation of the C-terminus (Tuzi et al., 1994, 1996a; Yamaguchi et al., 1998).

Fig. 2, *A–C*, demonstrates that the improved spectral resolution allows us to assign the signals to individual single Ala residues in a site-specific manner. The assignment of Ala^{126} and Ala^{196} is straightforward by comparison of peaks from the A126G and A196G mutants with those of the wild type, unless other significant conformational changes are induced at the site of the mutation by this site-directed mutagenesis. It appears that the two peaks at 17.38 (lower field peak of the doublet for the loop) and 16.88 ppm are shifted upfield to some extent to overlap with other peaks (Fig. 2 *B*). The former and latter peaks can be tentatively ascribed to Ala^{103} and Ala^{84} on the basis of ^{13}C NMR spectra of A103C and A84G, respectively (manuscript in preparation). Interestingly, in the structural model of Lu-ecke et al. (1998), there is van der Waals contact between the C_β carbon of Ala^{126} and the phenolic OH of Tyr^{83} (3.5 Å). This means that replacement of Ala^{126} with Gly may induce a slight conformational modification at the C and D helix and its interconnecting loops, which could result in the displacements of the peaks for Ala^{103} and Ala^{84}. These specifically assigned peaks, especially for Ala^{126} and Ala^{196}, will be utilized to identify a cation-binding site in this study. A local conformational change in the E194Q mutant in the extracellular region, especially at Ala^{126} and Ala^{196}, is suggested by downfield and upfield displacements of these peaks, respectively, relative to those of the wild type.

Comparison between purple and blue forms of bR

UV difference spectroscopy (Dunach et al., 1988a), Fourier transform infrared spectroscopy (Dunach et al., 1989), and solid-state NMR study of [4-^{13}C]Asp-labeled bR (Metz et al., 1992) have suggested that there is a conformational difference between the blue and purple forms of bR. In Fig. 3, CP-MAS spectra of the acid blue (pH 1.2) (Fig. 3 *B*) and the deionized blue (pH 4) (Fig. 3 *C*) forms are compared with the spectrum of the native purple form at neutral pH (Fig. 3 *A*). Most of the peaks in the deionized blue form, except for one peak at 16.20 ppm, were displaced as compared with those of the native purple form. Only a few

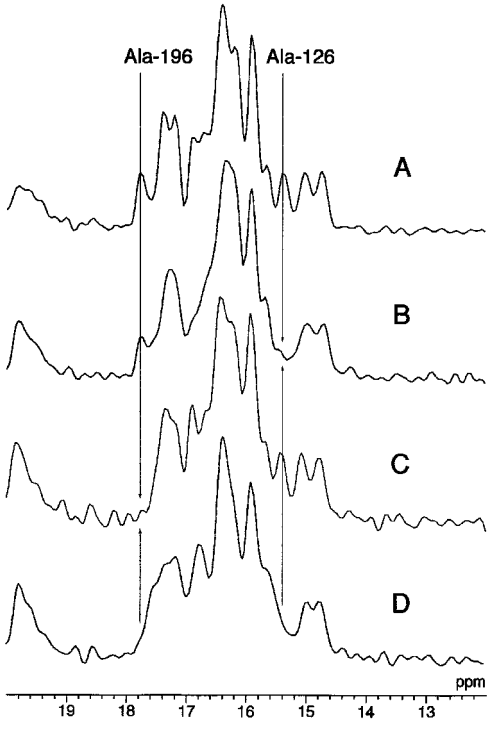

FIGURE 2 ^{13}C CP-MAS NMR spectra of [3-^{13}C]Ala-labeled wild-type bR (*A*) and its mutants at pH 7.0: A126G (*B*), A196G (*C*), and E194Q (*D*).

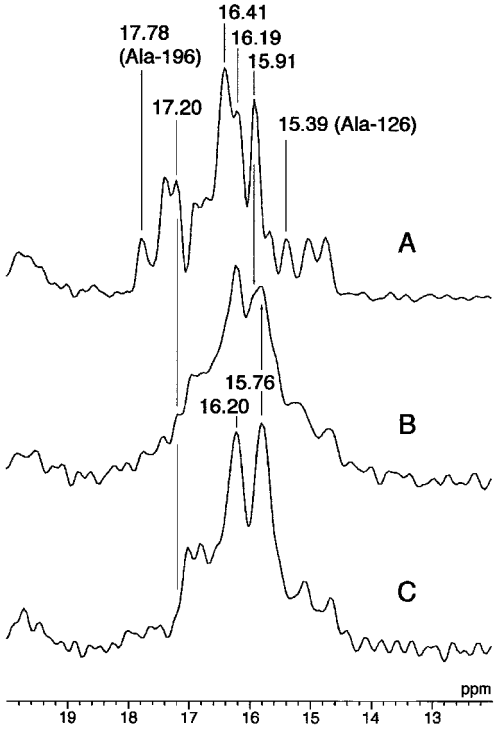

FIGURE 3 ^{13}C CP-MAS NMR spectra of [3-^{13}C]Ala-labeled native bR at neutral pH (*A*), its acid blue form at pH 1.2 (*B*), and its deionized blue form (pH 4) (*C*).

residues, corresponding to the peak at 16.20 ppm, which is from α_{II}-helix, might retain their native local conformation. The prominent spectral change from the purple to the blue form is the absence of peaks from the loop region (17.20, 17.38, and 17.78 (Ala^{196}) ppm). These peaks are shifted upfield, implying distinctive conformational changes. The intense peaks at 16.41 ppm and 15.91 ppm in the α_{II}-helix region in Fig. 3 *A* are shifted upfield to form a new peak at 15.76 ppm in the α_{II}-helix region. The three well-resolved peaks at the α_I-helix region of the native bR at 14.74, 15.02, and 15.39 ppm (attributed to Ala^{126}) are displaced to form the two peaks at 14.65 and 15.09 ppm upon deionization. The displacement of the peak for Ala^{126} suggests that the extracellular site of helix D is involved in conformational changes in the purple-to-blue transition. From DD-MAS spectra of the native and deionized bR (data not shown), the C-terminal tail taking a random coil conformation is found to be unaffected by deionization or lowering pH, because of the unchanged peak intensity or peak position at 16.87 ppm. The CP-MAS spectrum of the acid blue form (Fig. 1 *B*) shows changes similar to those of the deionized blue form, except for some characteristic peaks for the native conformation. The shoulder peaks at 15.90 and 17.14 ppm correspond to the peaks at 15.91 and 17.20 ppm of the native bR, and the broad peaks at 14.68 and 15.22 ppm seem to be an overlap of the peaks in the α_I-helix region of the native and the deionized forms.

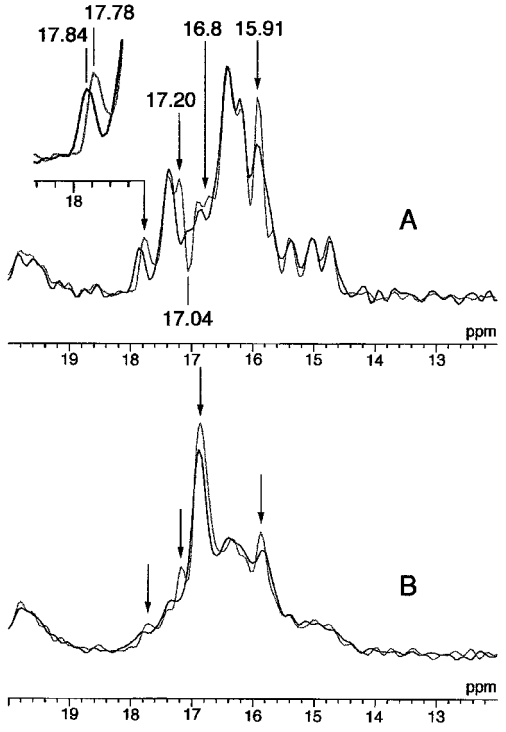

FIGURE 4 Comparison of ^{13}C CP-MAS (*A*) and DD-MAS (*B*) NMR spectra of bR at pH 7.0 between [3-^{13}C]Ala-labeled native purple form (*gray trace*) and Na^+ purple form (*black trace*).

Specific sites of cation bindings in bR at neutral pH

We adjusted the pH of the deionized blue membrane suspension to 7 by stepwise addition of NaOH. The absorption maximum of the deionized membrane recovered from 604 nm to the 568 nm of the native purple membrane, and the photoreaction cycle of purple membranes was restored. This membrane will be referred to as the Na^+ purple form.

In Fig. 4 CP-MAS and DD-MAS NMR spectra of the Na^+ purple form of bR (*black traces*) are superimposed on the spectra of the native purple form (*gray traces*). In contrast to the extensive spectral change observed for the acid and deionized blue forms, most of the peaks in the Na^+ purple form are almost the same as those of the native purple form, particularly in the α-helix region. It is noteworthy that most of the native conformation of the transmembrane helices is restored in the Na^+ purple form, as manifested from the restored peak positions. Only the four peaks designated in Fig. 4 by the arrows differ between the Na^+ and the native purple forms. These remaining changes between the Na^+ and the native purple forms are ascribed to a local conformational change near the specific cation-binding sites caused by replacement of divalent cation (Ca^{2+}, Mg^{2+}) with monovalent Na^+ ion. Interestingly, one of the changes induced by the substitution of the bound cations is a rather small but significant downfield displacement of the Ala^{196} peak from 17.78 ppm to 17.84 ppm (the digital resolution of the spectra is 0.025 ppm). This spectral change was well reproduced in the DD-MAS spectra (Fig. 4 *B*). This finding suggests that a high-affinity site for the divalent cation is near the F-G interhelical loop on the extracellular surface that includes Ala^{196}, as judged from its spectral change induced by the bound cation. It is also noteworthy that the peak indicated with an arrow at 17.20 ppm (loop) is shifted upfield by 0.16 ppm to 17.04 ppm by replacement of the bound cation. This spectral change is ascribed to the presence of an additional binding site of a cation to the loop in the cytoplasmic side, because there is no other Ala residue other than Ala^{196} in the extracellular loops. The reduced signal intensity around 16.8 ppm also seems to reflect a conformational change in the cytoplasmic side. The peak labeled with an arrow at 15.91 ppm in the α_{II}-helix region is suppressed to some extent by the transition from the native to the Na^+ purple form, as a result of conformational change and/or acquisition of motional freedom, which would interfere with the proton decoupling frequency.

We also utilized the carbonyl ^{13}C signal of Val^{199} of [1-^{13}C]Val-bR (at 171.11 ppm) assigned on the basis of comparison of peaks between wild-type (Fig. 5 *B*) and V199A (Fig. 5 *A*) as a probe to detect the conformational change induced by the replacement of the bound cation (Fig. 5 *C*), as illustrated in Fig. 5. Because Val^{199} is linked to Pro^{200}, it is expected that the peak of [1-^{13}C] Val^{199} will be shifted upfield by ~2.6 ppm (Torchia and Lyeria, 1974) from the usual conformation-dependent chemical shift

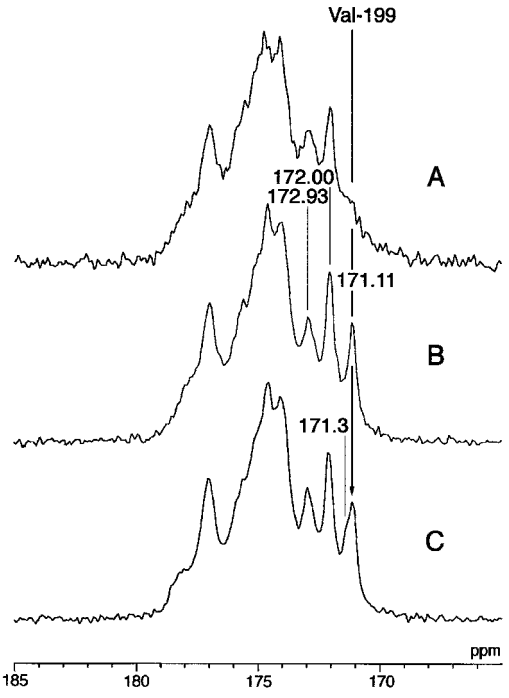

FIGURE 5 ^{13}C CP-MAS NMR spectra of [1-^{13}C]Val-labeled V199A mutant bR in the native purple membrane (*A*), wild-type bR in the native purple membrane (*B*) and wild-type bR in the Na^+ purple membrane (*C*) at pH 7.0.

(Saitô, 1986; Saitô and Ando, 1989). In a similar manner, the peaks at 172.00 and 172.93 ppm in a CP-MAS spectrum of [1-^{13}C]Val-labeled bR were assigned to Val^{49} and Val^{69}, respectively, by means of site-directed mutagenesis and an enzymatic cleavage experiment (unpublished). The observation of almost identical spectra of the native purple membrane (Fig. 5 *B*) as compared with the Na^+ purple membrane (Fig. 5 *C*) indicates that the conformation probed by the carbonyl carbons of Val residues is not sensitive to the replacement of the divalent cations by Na^+ ions, except for rather small changes of shoulders around 178 ppm and 171.3 ppm. Although the shoulder in the spectrum of the Na^+ purple membrane overlaps with the peak at 171.11 ppm assigned to Ala^{199}, the spectrum of the V199A mutant in the Na^+ purple membrane shows that the new peak at 171.42 ppm remains and must be attributed to residues other than Val^{199} (data not shown). The identical chemical shift and peak intensity of the peak at 171.11 ppm for the native and Na^+ purple membrane clearly indicate that the conformation of Val^{199}, only three residues from Ala^{196}, is not influenced by substitution of the cation at the binding site near Ala^{196}.

At present, it is not easy to completely rule out the possibility that the aforementioned NMR features of the Na^+ purple form are mainly caused by lower surface pH, because the Na^+ purple membrane preparation contains 400–650 μM NaOH instead of 5 mM HEPES buffer (pH 7.0) plus 10 mM NaCl and 0.025% NaN_3 in the native purple membrane preparation. For this reason, we tried to observe the specific cation-binding sites more directly by means of replacing Na^+ in the Na^+ purple membrane with Ca^{2+} and Mn^{2+}, because the latter ion is a paramagnetic relaxation reagent for NMR, causing line broadening or suppression of a peak when near the bound Mn^{2+}. This is feasible because Mn^{2+} can also regenerate a functional purple form from the deionized blue bR and shows almost the same stoichiometry and apparent affinity constants as Ca^{2+} in cation titration (Dunach et al., 1987, 1988a), although the binding sites themselves are shown to depend on the type of cations, such as lanthanide (Griffiths et al., 1996a,b; Roselli et al., 1996). The CP-MAS and DD-MAS spectra of the Na^+ purple membrane treated with 5 μM $CaCl_2$ (Fig. 6 *A*; hereafter referred to as a Ca^{2+} purple membrane) show characteristics intermediate between those of the native purple form and the Na^+ purple form. The broadened peak at 15.91 ppm in the spectra of the Na^+ purple form becomes narrower and approaches the line shape in the spectra of the native purple membrane by Ca^{2+} treatment. An increase in the peak intensity at 17.11 ppm, coupled with a decrease in intensity at 17.04 ppm induced by the Ca^{2+} treatment, indicates a reverse shift of the peak downfield to restore the peak at 17.20 ppm in the spectra of the native purple membrane. This spectral change can be ascribed to a recovery of the structured C-terminus involving the α-helix conformation from the presence of the divalent cations at the cytoplasmic site, although further work will be necessary to prove this. The peak assigned to Ala^{196} seems to be also shifted slightly upfield, but the chemical shift change induced by the Ca^{2+} treatment from 17.84 to 17.80 ppm is not significant, considering the digital resolution of the spectra.

In Fig. 6 *B*, CP-MAS and DD-MAS spectra of the Na^+ purple membrane treated with 5 μM $MnCl_2$ (*black trace*; hereafter referred to as Mn^{2+} purple membrane) are shown superimposed on the spectra of the Ca^{2+} purple membrane (*gray trace*). The peak intensity of those spectra is normalized at the peaks of 16.17 ppm to make intensity of the peaks in the spectra of the Mn^{2+} purple form equal to or less than that of the corresponding peaks in the spectra on the Ca^{2+} purple form. This normalization is performed for the convenient comparison of the relative extents of reductions of the peaks induced by Mn^{2+}. It should be noted that the five peaks are completely or partially suppressed by the presence of Mn^{2+} ion (designated by *arrows*), including the peaks (at 15.88, 17.11, and 17.80 ppm) affected by the replacement of divalent cation with Na^+. The peaks at 16.18, 15.41, 15.04, and 14.71 ppm in the α_I- and α_{II}-helix regions are relatively unaffected by Mn^{2+}, consistent with their insensitivity to the replacement of divalent cation with Na^+. Such selective suppression of the peaks by Mn^{2+} implies that there are high-affinity Mn^{2+} binding sites in bR, and only some of them relate to the conformational change of bR induced by the replacement of the binding divalent cations by Na^+. Any possibility that the selective peak suppression is caused by interactions between free Mn^{2+} ions in the medium and residues on the hydrophilic

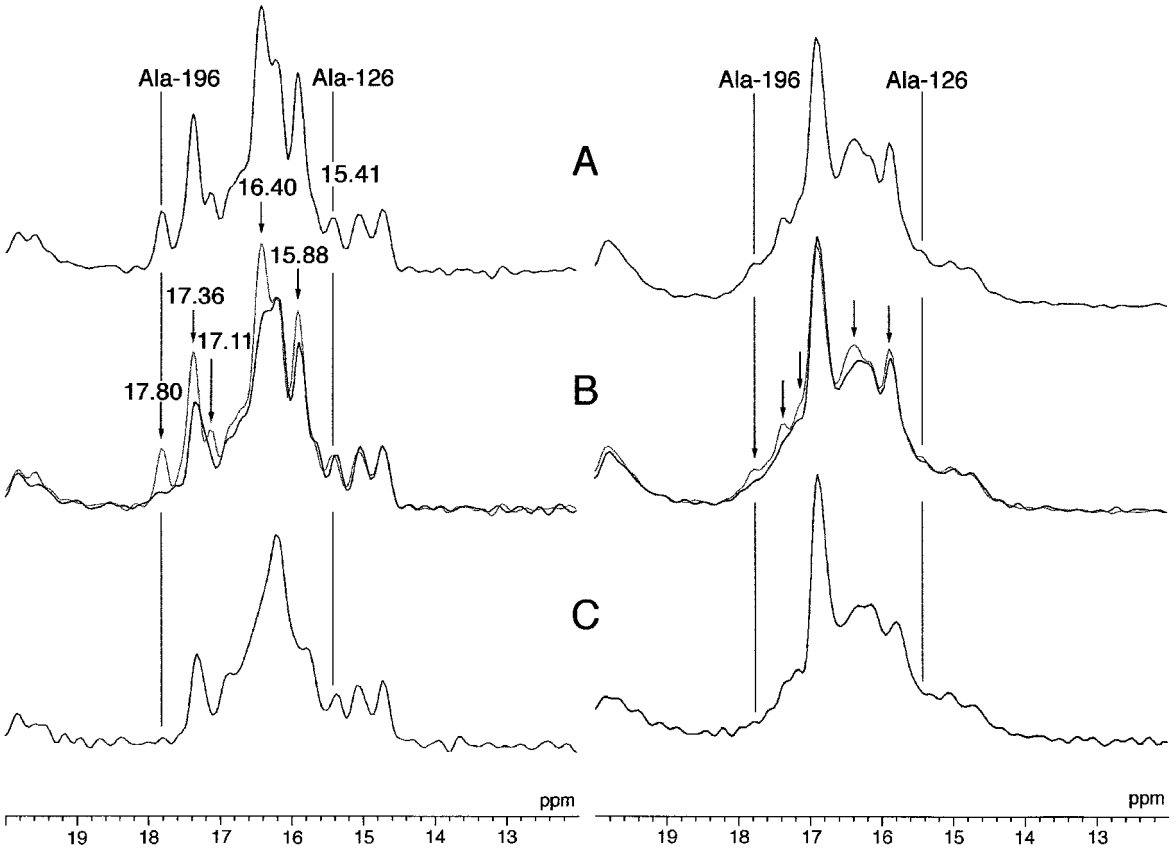

FIGURE 6 ^{13}C CP-MAS (*left*) and DD-MAS (*right*) NMR spectra of [3-^{13}C]Ala-labeled deionized purple membrane treated with 5 μM Ca^{2+} (*A*), 5 μM Mn^{2+} (*black trace*) or 5 μM Ca^{2+} (*gray trace*) (*B*) and 30 μM Mn^{2+} (*C*) at pH 7.0.

surface of the protein is ruled out, because the peak at 16.88 ppm in the DD-MAS spectra (Fig. 6 *B*, *right*), attributed to the extramembrane C-terminus, which is exposed to medium, is unaffected by Mn^{2+}.

Among others, the Ala^{196} peak at 17.80 ppm is strongly suppressed in the Mn^{2+} purple form (Fig. 6 *B*), which is treated with 5 μM $MnCl_2$, and completely disappears when the Na^+ purple membrane is treated with 30 μM $MnCl_2$ (Fig. 6 *C*). This finding implies that one of the high-affinity binding sites for cations lies at the extracellular side located near Ala^{196}. The observation of additional sites for the suppressed peaks at 17.11 ppm (loop) and 15.88 ppm (α_{II}-helix) shows that cation-binding sites are also located at the cytoplasmic surface or at the transmembrane helices. In contrast, no spectral change was induced for the peaks at 16.7–16.9 ppm of the Mn^{2+} purple membrane. There might be two explanations for this inconsistency: 1) the conformations of the Ala residues corresponding to these peaks are affected by distant cation- binding sites, 2) the changes in these peaks observed for the Na^+ purple form are caused by differences in surface pH between the native and the Na^+ purple membranes. The peaks at 17.36 and 16.40 ppm in the spectra of the Ca^{2+} purple form are strongly suppressed in the spectra of the Mn^{2+}-treated form, despite the insensitivity of these peaks to the replacement of the cations by Na^+. These peaks can be ascribed to Ala residues in the cytoplasmic loops and transmembrane helices near the cation-binding sites, respectively, whose conformations are unaffected by bound cations.

These spectral changes were induced by the addition of Mn^{2+} despite the low amount of Mn^{2+} in the Mn^{2+} purple membrane (the mole ratio of Mn^{2+} to bR is less than 1/10 in the preparation treated with 5 μM $MnCl_2$), indicating the presence of rapid exchange of the divalent cations among the bR molecules and the cation-binding sites in a single molecule. The possibility that the Mn^{2+} ion is strongly bound to a single binding site without exchange is easily ruled out, in view of the low concentration of Mn ion (1/10 to bR). In Fig. 6 *B*, the peak of Ala^{196} in the CP-MAS spectrum is reduced by Mn^{2+} to less than 25% of the peak intensity in the spectra of the Ca^{2+} purple form, and at least five different peaks corresponding to the different residues present on both the cytoplasmic and extracellular sides are substantially suppressed simultaneously by Mn^{2+}. Therefore, through an inter- and intramolecule exchange of cations in the purple membrane, at least 75% of the bR molecules and the several binding sites in the individual bR molecules seem to be affected, apparently simultaneously, by a small amount of Mn^{2+}. The exchange is estimated to be at least as rapid as 3 ms, judging from the linewidth. The extent of the reduction of the peaks at 16.40 and 15.88 ppm is substantially larger in the Mn^{2+} purple membrane treated

with 30 μM $MnCl_2$ (Fig. 6 *C*) than in the preparation treated with 5 μM $MnCl_2$ (Fig. 6 *B*). These peaks seem to be related to the cation binding sites with relatively low affinity as compared with the site near Ala^{196}, which induces substantial suppression of Ala^{196}, even when the purple membrane is treated with 5 μM Mn^{2+}.

DISCUSSION

Conformational change induced by the purple-to-blue transition

We report evidence for a major conformational change associated with the color change from the purple to the blue form, from a substantial NMR spectral change (Fig. 3). This means that the conformation and/or dynamics of the deionized blue form of bR are significantly altered from those of the native purple form. In addition, we find that the two types of blue forms, deionized blue (pH 4) and acid blue (pH 1.2), are identical in their spectra as a result of lowered surface pH, consistent with the previous works by Szundi and Stoeckenius (1987, 1989) and Jonas and Ebrey (1991). Adjusting the bulk pH of the deionized blue membrane from pH 4 to pH 7 resulted in recovery of the major spectral change (although incomplete), the absorption maximum, and the photocycle. Considering this structural difference, it can be expected that the binding sites found during titration of deionized blue membrane, especially at high-affinity cation-binding sites occupied at low concentration of cations, are not identical to those of the purple membrane.

In this connection, caution should be used in referring to some observed phenomena as cation binding, such as high-affinity and low-affinity bindings based on Ca^{2+}-selective electrode studies (Zhang et al., 1992, 1993; Zhang and El-Sayed, 1993; Yang and El-Sayed, 1995; Yoo et al., 1995), spectroscopic titration (Ariki and Lanyi, 1986), electron spin resonance (Dunach et al., 1987), radioactive $^{45}Ca^{2+}$ (Dunach et al, 1988b), fluorescence intensity of $Ru(bpy)_3^{2+}$ (Wu and El-Sayed, 1994a), 3,6-diaminoacridine cation (DAA^+)(Wu and El-Sayed, 1994b), and Eu^{3+} (Sweetman and El-Sayed, 1991), because there is a possibility that some of these data may be related to cation-induced pH changes. This is because the cation-binding sites in the deionized blue form may be different from those in the purple form. For this reason, these should be referred to as the cation-binding sites of the blue form.

The present NMR study shows that the bound cations are not strongly bound, but undergo exchange among several sites with an estimated rate greater than 3×10^2 s^{-1}. This result is consistent with that of the electron diffraction study for the Pb^{2+}-regenerated bR, which has suggested that the regenerated purple membrane contains two Pb^{2+} ions, and the identified six cation-binding sites are partially occupied (0.24–0.55 Pb^{2+} equivalents) by Pb^{2+} (Mitra and Stroud, 1990). A study of emission lifetimes of bound Eu^{3+} in the Eu^{3+}-regenerated purple membrane has also shown equivalent binding constants for Eu^{3+} ions corresponding to three observed decay components of emission (Corcoran et al., 1987). The rapid exchange of the cations observed in this study seems to be consistent with the finding that the cation-binding sites are located on the surface (Mitra and Stroud, 1990; Fu et al., 1997; Engelhard et al., 1989), even though the changes in the peaks at 15.88 ppm and 16.40 ppm for the Mn^{2+} and Na^+ purple membrane show that parts of the α_{II}-helices are close to the cation-binding sites. Thus, although the findings in this study do not rule out the possibility of cation-binding sites in the transmembrane region of bR, we expect from the NMR results that the cation-binding sites are near the hydrophilic surface and thus are easily accessible to the medium. The same conclusion was made from a study of the accessibility of large cations to the binding site, which confers a spectral shift on the deionized blue membrane (Fu et al., 1997).

Specific sites for cation binding

As shown in the Results, one of the preferred cation-binding sites was located to a portion close to Ala^{196} in the F-G loop on the extracellular surface. Interestingly, the Ala^{126} peak of the helix D at the extracellular surface was unaffected by the replacement of the cation with Na^+ or by treatment with Mn^{2+}, suggesting that this residue is distant from the cation-binding site near Ala^{196}. One of the candidates for ligands in the cation-binding site near Ala^{196} is the side-chain carboxyl group of Glu^{194} in the F-G loop. The currently available 3D structures, from cryoelectron microscopy (Grigorieff et al., 1996) and x-ray diffraction (Luecke et al., 1998), indicate the possibility of Coulombic interaction between Glu^{194} in the F-G loop and Arg^{134} in helix E. The present NMR study on the E194Q mutant, in which the negative charge of Glu^{194} is removed, is consistent with such interaction, exhibiting shifts of the Ala^{196} and Ala^{126} peaks relative to the wild type (Fig. 2 *D*). In Fig. 7, the distances between the side-chain carboxyl carbon of Glu^{194} and the side-chain

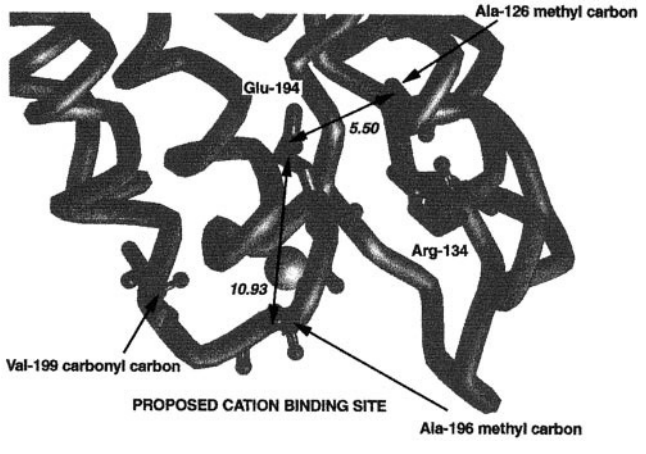

FIGURE 7 A proposed cation (shown as a large sphere) binding site at the F-G loop. The structure is from the coordinates from an x-ray diffraction study by Luecke et al. (1998).

methyl carbons of these alanine residues are shown as 5.50 Å for Ala^{126} and 10.93 Å for Ala^{196} (Luecke et al., 1998). If Mn^{2+} binds to the side chain of Glu^{194}, the NMR peak of Ala^{126} is expected to be suppressed, as is the peak of Ala^{196}. Thus we conclude that a variety of ligands other than Glu^{194} may form the cation-binding site near Ala^{196}, presumably peptide carbonyl groups in the C-terminus of the helix F and the F-G loop. The displacement of the peak of Ala^{196} induced by the replacement of the cation with Na^+ suggests a structural role of the bound cation at this site in forming the native conformation of the loop in the vicinity of Ala^{196}. In contrast, the NMR spectrum of Val^{199} is unaffected by the replacement of the cations with Na^+. This supports the location of the cation-binding site at the part of the F-G loop near the C-terminus of helix F, as shown in Fig. 7. The structural model of the cation-binding site includes only oxygens of carbonyl groups in the backbone and water molecules as the ligands of the bound cation. This kind of cation-binding site is consistent with the structures of the cation-binding sites proposed by x-ray absorption studies, which are suggested to include oxygen atoms as ligands (Zhang et al., 1997; Engelhard et al., 1987; Sepulcre et al., 1996).

The changes in the NMR peaks upon substitution of the binding cations also implies the presence of cation-binding sites in the loops located on the cytoplasmic side and the α-helix region. In both the loop and α-helix regions, two different kinds of residues close to the cation-binding sites are found: 1) residues whose torsion angles are affected by the substitution of cations and 2) residues whose torsion angles are unaffected by the substitution of cations. This difference might reflect the nature of the contribution of the bound cations to the conformation of the protein. Although the presence of the cation-binding sites near the α-helix region might correspond to the cation-binding sites in the interior, the rather high exchange rate of the binding cations and the insensitivity of the conformations of the transmembrane α-helices, except those that resonate at 15.91 ppm, on the replacement of the divalent cations by the monovalent Na^+ ions, seem to imply that the α-helices close to the cation-binding sites are located on the surface, being the termini of the transmembrane helices and the α-helix in the C-terminus (Yamaguchi et al., 1998). Because assignment of the peaks of the alanine residues present on the cytoplasmic surface and the transmembrane α-helix region is still in progress, we can only conclude at present that more than one cation-binding site is located on the cytoplasmic surface of bR, and the sites have structural roles in assembling part of the loops and α-helices, allowing them to assume their native conformation.

The major advantage of the ^{13}C NMR probe is to be able to locate the most probable site for cation binding as viewed from the protein side. It is pointed out, however, that conformation changes occurring as a result of metal cation substitution could also occur elsewhere and not necessarily near Ala or Val, causing changes in the NMR spectrum. Therefore, it is true that the current NMR approach does not always completely exclude the possibility of the presence of sites in the interior of bR, as in the vicinity of Asp^{85}, if they can undergo a rapid exchange process.

This work was partially supported by a Grant in Aid for Scientific Research from the Ministry of Education, Science, Culture, and Sports of Japan (09780610, 09480179, 09558094, 09261233, and 10157220).

REFERENCES

Ariki, M., and J. K. Lanyi. 1986. Characterization of metal ion-binding sites in bacteriorhodopsin. *J. Biol. Chem.* 261:8167–8174.

Brown, L. S., J. Sasaki, H. Kandori, A. Maeda, R. Needleman, and J. K. Lanyi. 1995. Glutamic acid 204 is the terminal proton release group at the extracellular surface of bacteriorhodopsin. *J. Biol. Chem.* 270: 27122–27126.

Chang, C. H., J. G. Chen, R. Govindjee, and T. Ebrey. 1985. Cation binding by bacteriorhodopsin. *Proc. Natl. Acad. Sci. USA.* 82:396–400.

Chang, C. H., R. Jonas, S. Melchiore, R. Govindjee, and T. G. Ebrey. 1986. Mechanism and role of divalent cation binding of bacteriorhodopsin. *Biophys. J.* 49:731–739.

Corcoran, T. C., K. Z. Ismail, and M. A. El-Sayed. 1987. Evidence for the involvement of more than one metal cation in the Schiff base deprotonation process during the photocycle of bacteriorhodopsin. *Proc. Natl. Acad. Sci. USA.* 84:4094–4098.

Dioumaev, A. K., H. T. Richter, L. S. Brown, M. Tanio, S. Tuzi, H. Saitô, Y. Kimura, R. Needleman, and J. K. Lanyi. 1998. Existence of a proton transfer chain in bacteriorhodopsin: participation of Glu-194 in the release of protons to the extracellular surface. *Biochemistry.* 37: 2496–2506.

Dunach, M., E. Padrós, A. Muga, and J. L. Arrondo. 1989. Fourier-transform infrared studies on cation binding to native and modified purple membranes. *Biochemistry.* 28:8940–8945.

Dunach, M., E. Padrós, M. Seigneuret, and J. L. Rigaud. 1988a. On the molecular mechanism of the blue to purple transition of bacteriorhodopsin. *J. Biol. Chem.* 263:7555–7559.

Dunach, M., M. Seigneuret, J. L. Rigaud, and E. Padrós. 1988b. Influence of cations on the blue to purple transition of bacteriorhodopsin. *J. Biol. Chem.* 263:17378–17384.

Dunach, M., M. Seigneuret, J. L. Rigaud, and E. Padrós. 1987. Characterization of the cation binding sites of the purple membrane. Electron spin resonance and flash photolysis studies. *Biochemistry.* 26:1179–1186.

Engelhard, M., B. Hess, M. Chance, and B. Chance. 1987. X-ray absorption studies on bacteriorhodopsin. *FEBS Lett.* 222:275–278.

Engelhard, M., B. Pevec, and B. Hess. 1989. Modification of two peptides of bacteriorhodopsin with a pentaamminecobalt(III) complex. *Biochemistry.* 28:5432–5438.

Fischer, U., and D. Oesterhelt. 1979. Chromophore equilibria in bacteriorhodopsin. *Biophys. J.* 28:211–230.

Fu, X., S. Bressler, M. Ottolenghi, T. Eliash, N. Friedman, and M. Sheves. 1997. Titration kinetics of Asp-85 in bacteriorhodopsin: exclusion of the retinal pocket as the color-controlling cation binding site. *FEBS Lett.* 416:167–170.

Griffiths, J. A., M. A. El-Sayed, and M. Capel. 1996a. Effect of binding of lanthanide ions on bacteriorhodopsin hexagonal structure: an x-ray study. *J. Phys. Chem.* 100:12002–12007.

Griffiths, J. A., T. M. Masciangioli, C. Roselli, and M. A. El-Sayed. 1996b. Mono-dentate vs. bidentate binding of lanthanide cations to PO_2^- in bacteriorhodopsin. *J. Phys. Chem.* 100:6863–6866.

Grigorieff, N., T. A. Ceska, K. H. Downing, J. M. Baldwin, and R. Henderson. 1996. Electron-crystallographic refinement of the structure of bacteriorhodopsin. *J. Mol. Biol.* 259:393–421.

Jonas, R., and T. G. Ebrey. 1991. Binding of a single divalent cation directly correlates with the blue-to-purple transition in bacteriorhodopsin. *Proc. Natl. Acad. Sci. USA.* 88:149–153.

Kimura, Y., A. Ikegami, and W. Stoeckenius. 1984. Salt and pH-dependent changes of the purple membrane absorption spectrum. *Photochem. Photobiol.* 40:641–646.

Lanyi, J. K. 1993. Proton translocation mechanism and energetics in the light-driven pump bacteriorhodopsin. *Biochim. Biophys. Acta.* 1183: 241–261.

Lanyi, J. K. 1997. Mechanism of ion transport across membranes. Bacteriorhodopsin as a prototype for proton pumps. *J. Biol. Chem.* 272: 31209–31212.

Luecke, H., H. T. Richter, and J. K. Lanyi. 1998. Proton transfer pathways in bacteriorhodopsin at 2.3 angstrom resolution. *Science.* 280: 1934–1937.

Mathies, R. A., S. W. Lin, J. B. Ames, and W. T. Pollard. 1991. From femtoseconds to biology: mechanism of bacteriorhodopsin's light-driven proton pump. *Annu. Rev. Biophys. Biophys. Chem.* 20:491–518.

Metz, G., F. Siebert, and M. Engelhard. 1992. Asp^{85} is the only internal aspartic acid that gets protonated in the M intermediate and the purple-to-blue transition of bacteriorhodopsin. *FEBS Lett.* 303:237–241.

Mitra, A. K., and R. M. Stroud. 1990. High sensitivity electron diffraction analysis. A study of divalent cation binding to purple membrane. *Biophys. J.* 57:301–311.

Moore, T. A., M. E. Edgerton, G. Parr, C. Greenwood, and R. N. Perham. 1978. Studies of an acid-induced species of purple membrane from *Halobacterium halobium. Biochem. J.* 171:469–476.

Mowery, P. C., R. H. Lozier, Q. Chae, Y. Tseng, M. Taylor, and W. Stoeckenius. 1979. Effect of acid pH on the absorption spectra and photoreactions of bacteriorhodopsin. *Biochemistry.* 18:4100–1407.

Oesterhelt, D., and W. Stoeckenius. 1974. Isolation of the cell membrane of *Halobacterium halobium* and its fractionation into red and purple membrane. *Methods Enzymol.* 31:667–678.

Onishi, H., M. E. McCance, and N. E. Gibbons. 1965. A synthetic medium for extremely halophilic bacteria. *Can. J. Microbiol.* 11:365–373.

Ovchinnikov, Y. A. 1982. Rhodopsin and bacteriorhodopsin: structure-function relationships. *FEBS Lett.* 148:179–191.

Roselli, C., A. Boussac, T. A. Mattioli, J. A. Griffiths, and M. A. El-Sayed. 1996. Detection of a Yb^{3+} binding site in regenerated bacteriorhodopsin that is coordinated with the protein and phospholipid head groups. *Proc. Natl. Acad. Sci. USA.* 93:14333–14337.

Saitô, H. 1986. Conformation-dependent ^{13}C chemical shifts: a new means of conformational characterization as obtained by high-resolution solid-state NMR. *Magn. Reson. Chem.* 24:835–852.

Saitô, H., and I. Ando. 1989. High-resolution solid-state NMR studies of synthetic and biological macromolecules. *Annu. Rep. NMR Spectrosc.* 21:209–290.

Sepulcre, F., J. Cladera, J. Garcia, M. G. Proietti, J. Torres, and E. Padrós. 1996. An extended x-ray absorption fine structure study of the high-affinity cation-binding site in the purple membrane. *Biophys. J.* 70: 852–856.

Stoeckenius, W., and R. A. Bogomolni. 1982. Bacteriorhodopsin and related pigments of halobacteria. *Annu. Rev. Biochem.* 52:587–616.

Subramaniam, S., T. Marti, and H. G. Khorana. 1990. Protonation state of Asp (Glu)-85 regulates the purple-to-blue transition in bacteriorhodopsin mutants Arg-82—Ala and Asp-85—Glu: the blue form is inactive in proton translocation. *Proc. Natl. Acad. Sci. USA.* 87:1013–1017.

Sweetman, L. L., and M. A. El-Sayed. 1991. The binding site of the strongly bound Eu^{3+} in Eu^{3+}-regenerated bacteriorhodopsin. *FEBS Lett.* 282:436–440.

Szundi, I., and W. Stoeckenius. 1987. Effect of lipid surface charges on the purple-to-blue transition of bacteriorhodopsin. *Proc. Natl. Acad. Sci. USA.* 84:3681–3684.

Szundi, I., and W. Stoeckenius. 1989. Surface pH controls purple-to-blue transition of bacteriorhodopsin. *Biophys. J.* 56:369–383.

Tanio, M., S. Tuzi, S. Yamaguchi, H. Konishi, A. Naito, R. Needleman, J. K. Lanyi, and H. Saitô. 1998. Evidence of local conformational fluctuations and changes in bacteriorhodopsin, dependent on lipids, detergents and trimeric structure, as studied by ^{13}C NMR. *Biochim. Biophys. Acta.* 1375:84–92.

Torchia, D. A., and J. R. Lyeria, Jr. 1974. Molecular mobility of polypeptides containing proline as determined by ^{13}C magnetic resonance. *Biopolymers.* 13:97–114.

Tuzi, S., A. Naito, and H. Saitô. 1993. A high-resolution solid-state ^{13}C-NMR study on [1-^{13}C]Ala and [3-^{13}C]Ala and [1-^{13}C]Leu and Val-labelled bacteriorhodopsin. *Eur. J. Biochem.* 218:837–844.

Tuzi, S., A. Naito, and H. Saitô. 1994. ^{13}C NMR study on conformation and dynamics of the transmembrane α-helices, loops, and C-terminus of [3-^{13}C]Ala-labeled bacteriorhodopsin. *Biochemistry.* 33:15046–15052.

Tuzi, S., A. Naito, and H. Saitô. 1996a. Temperature-dependent conformational change of bacteriorhodopsin as studied by solid-state ^{13}C NMR. *Eur. J. Biochem.* 239:294–301.

Tuzi, S., S. Yamaguchi, A. Naito, R. Needleman, J. K. Lanyi, and H. Saitô. 1996b. Conformation and dynamics of [3-^{13}C]Ala-labeled bacteriorhodopsin and bacterioopsin, induced by interaction with retinal and its analogs, as studied by ^{13}C nuclear magnetic resonance. *Biochemistry.* 35:7520–7527.

Wu, S., and M. A. El-Sayed. 1994a. Binding characteristics of an organometallic cation, $Ru(bpy)_3^{2+}$, in regenerated bacteriorhodopsin. *J. Phys. Chem.* 98:7246–7251.

Wu, S., and M. A. El-Sayed. 1994b. Binding of, and energy-transfer studies from retinal to, organic cations in regenerated reduced bacteriorhodopsin. *J. Phys. Chem.* 98:9339–9344.

Yamaguchi, S., S. Tuzi, T. Seki, M. Tanio, R. Needleman, J. K. Lanyi, A. Naito, and H. Saitô. 1998. Stability of the C-terminal a-helical domain of bacteriorhodopsin that protrudes from the membrane surface, as studied by high-resolution solid-state ^{13}C NMR. *J. Biochem. (Tokyo).* 123: 78–86.

Yang, D., and M. A. El-Sayed. 1995. The Ca^{2+} binding to deionized monomerized and to retinal removed bacteriorhodopsin. *Biophys. J.* 69:2056–2059.

Yoo, S. K., E. S. Awad, and M. A. El-Sayed. 1995. Comparison between the binding of Ca^{2+} and Mg^{2+} to the two high-affinity sites of bacteriorhodopsin. *J. Phys. Chem.* 99:11600–11604.

Zhang, K., L. Song, J. Dong, and M. A. El-Sayed. 1997. Studies of cation binding in $ZnCl_2$-regenerated bacteriorhodopsin by x-ray absorption fine structures: effects of removing water molecules and adding Cl^- ions. *Biophys. J.* 73:2097–2105.

Zhang, Y. N., and M. A. El-Sayed. 1993. The C-terminus and the Ca^{2+} low-affinity binding sites in bacteriorhodopsin. *Biochemistry.* 32: 14173–14175.

Zhang, Y. N., M. A. El-Sayed, M. L. Bonet, J. K. Lanyi, M. Chang, B. Ni, and R. Needleman. 1993. Effects of genetic replacements of charged and H-bonding residues in the retinal pocket on Ca^{2+} binding to deionized bacteriorhodopsin. *Proc. Natl. Acad. Sci. USA.* 90:1445–1449.

Zhang, Y. N., L. L. Sweetman, E. S. Awad, and M. A. El-Sayed. 1992. Nature of the individual Ca^{2+} binding sites in Ca^{2+}-regenerated bacteriorhodopsin. *Biophys. J.* 61:1201–1206.